A Letters Journal Exploring the Frontiers of Physics

January 2025

EPL, **149** (2025) 15001
www.epljournal.org
doi: 10.1209/0295-5075/ada1f2

Optimal ion shuttling for a noisy trap

Xiao-Jing Lu[1(a)] and J. G. Muga[2,3]

[1] *School of Science, Xuchang University - Xuchang 461000, China*
[2] *EHU Quantum Center, University of the Basque Country UPV/EHU - Apdo. 644, 48080 Bilbao, Spain*
[3] *IUDEA, Universidad de la Laguna - Apdo. 456, 38205 La Laguna, Spain*

received 26 September 2024; accepted in final form 20 December 2024
published online 7 January 2025

Abstract – We find continuous optimal trap trajectories to shuttle one ion with minimal excitation, when the trap spring constant is affected by white noise. The Euler-Lagrange method gives a lower bound for the dynamical (trajectory-dependent) energy sensitivity to the noise. Using a trigonometric ansatz for the state trajectories, the optimal trap trajectories are found for a given shuttling time and a fixed number of terms in the ansatz. The corresponding dynamical sensitivity tends to the lower bound as the number of terms increases. While the dynamical sensitivity increases by shortening the shuttling times, the static (trajectory-independent) one decreases, so we also find optimal shuttling times that minimize the global (static plus dynamical) sensitivity.

Introduction. – Ion shuttling is a basic operation for fundamental physics research and quantum technologies [1–10]. In applications such as quantum computing [9–15], quantum sensors, or metrology [16–22], the challenge is to move the ions quickly without excitations or environmental decoherence. Adiabatic shuttling by slowly moving the trap could in principle lead to excitation-free transport but the long times involved make it impractical or prone to decoherence in most applications, which can be caused by different mechanisms such as voltage fluctuations. Shortcuts to adiabaticity (STA) [23,24] are techniques to achieve the results of a slow adiabatic evolution fast. They have attracted much attention to implement different operations in quantum technologies and specifically for ion or neutral-atom shuttling [25–36].

Recently, several works have applied STA methods to deliver the particles fast and motionally unexcited at destination considering the influence of environmental noise and systematic errors [36–42]. Lu *et al.* [38], in particular, applied the "invariant-based" inverse engineering method to design the trap trajectories and studied the influence of noise in the spring constant of the trap during single-ion shuttling. In combination with time-dependent perturbation theory, ref. [38] provides expressions for static (independent of the trap trajectory) and dynamical (dependent on transport path) energy sensitivities to the noise. Similarly, the effect of noise in different parameters for atomic transport in an optical lattice is studied in ref. [39]. These two papers use polynomial ansatzes for the state trajectories, and do not carry out any optimization. Espinós *et al.* [40] also use an invariant-based inverse technique to analyze the influence of systematic oscillating (rather than noisy) perturbations on the excitation energy, and optimize different transport schemes. Lu *et al.* [37] found optimal discontinuous trap trajectories for spring constant noise using optimal control and a master equation limited to short noise correlation times. In the present work we also optimize the trap trajectory for white noise in the spring constant, but, unlike [37], we look for continuous trajectories and the treatment can be extended to arbitrary correlation times.

First we review the invariant-based inverse engineering of the trap trajectories, and the lower bound for the sensitivity for white noise in the spring constant. A trigonometric ansatz for the state trajectory is used to inverse engineer continuous trap trajectories. They are optimized for minimal dynamical sensitivity to the noise for a given shuttling time and for a given number of terms. It is shown that as the number of terms increases, the sensitivity tends to the lower bound; After the final discussion, an appendix

(a)E-mail: luxiaojing1013@163.com (corresponding author)

extends the treatment to non-zero noise correlation times.

Invariant-based inverse engineering. – First, the invariant-based inverse engineering of the trap trajectory to shuttle an ion is reviewed [26]. We consider a harmonic trap with angular frequency $\Omega(t)$ for an ion of mass m. If the trap moves along $q_0(t)$, the Hamiltonian takes the form

$$H(t)=\frac{p^2}{2m}+\frac{1}{2}m\Omega^2(t)[x-q_0(t)]^2. \tag{1}$$

This Hamiltonian has the following invariant [26,43–45]:

$$\begin{aligned}I(t)\;=\;&\frac{1}{2m}\{\rho(t)[p-m\dot{q}_c(t)]-m\dot{\rho}(t)[x-\dot{q}_c(t)]\}^2\\&+\frac{1}{2}m\omega_0^2\left[\frac{x-q_c(t)}{\rho(t)}\right]^2,\end{aligned} \tag{2}$$

where $\rho(t)$ is a scaling factor for the width of the eigenstates of I and $q_c(t)$ is their center. The invariant $I(t)$ satisfies

$$\frac{\mathrm{d}I(t)}{\mathrm{d}t}\equiv\frac{\partial I(t)}{\partial t}+\frac{1}{i\hbar}[I(t),H(t)]=0, \tag{3}$$

provided that the functions $\rho(t)$ and q_c satisfy the "Ermakov" and "Newton" auxiliary equations,

$$\begin{aligned}&\ddot{\rho}(t)+\Omega^2(t)\rho=\frac{\omega_0^2}{\rho^3(t)},\\&\ddot{q}_c(t)+\Omega^2(t)q_c(t)=\Omega^2(t)q_0(t).\end{aligned} \tag{4}$$

The solutions of the time-dependent Schrödinger equation $i\hbar\partial_t\Psi(x,t)=H_0(t)\Psi(x,t)$ are superpositions of "transport modes" $\Psi_n(x,t)\equiv e^{i\theta_n(t)}\psi_n(x,t)$, where $\psi_n(t)$ are the (orthogonal) eigenstates of the invariant, $I(t)\psi_n(t)=\lambda_n\psi_n(t)$, and $\theta_n(t)$ are Lewis-Riesenfeld phases. The eigenvalues λ_n of $I(t)$ are constant, and $\psi_n(t)$ and $\theta_n(t)$ are given by [39]

$$\psi_n(x,t)=\frac{1}{\sqrt{\rho}}e^{\frac{im}{\hbar}[\frac{\dot{\rho}x^2}{2\rho}+\frac{(\dot{q}_c\rho-\dot{\rho}q_c)x}{\rho}]}\phi_n\left(\frac{x-q_c}{\rho}\right), \tag{5}$$

and

$$\theta_n(t)=\frac{1}{\hbar}\int_0^t\left\langle\psi_n(t')\middle|i\hbar\frac{\partial}{\partial t'}-H_0(t')\middle|\psi_n(t')\right\rangle\mathrm{d}t'. \tag{6}$$

The $\psi_n(t)$ are also eigenstates of H at initial and final times if H and I commute at those times, leading to excitation-free transport in which the n-th initial eigenstate of H becomes the n-th final eigenstate. The following boundary conditions achieve that goal [26]:

$$\begin{aligned}&q_c(0)=0,\quad q_c(t_f)=d,\\&\dot{q}_c(0)=0,\quad \dot{q}_c(t_f)=0.\end{aligned} \tag{7}$$

To make q_0 continuous at the time boundaries, the additional conditions

$$\ddot{q}_c(0)=0,\quad \ddot{q}_c(t_f)=0 \tag{8}$$

are also needed. We shall from now on demand in general that the six conditions in eqs. (7) and (8) are satisfied, except for calculating a bound for the possible excitations.

For a rigid harmonic trap we may simply set

$$\Omega(t)=\omega_0,\quad \rho(t)=1, \tag{9}$$

but in the following we shall assume a perturbing noise in the spring constant.

Noise sensitivity. – Now we consider a classical spring constant noise $\Omega^2(t)=\omega_0^2[1+\lambda\xi(t)]$. λ is a dimensionless perturbative parameter that should be set to one at the end of the calculation, and the noise function $\xi(t)$ is also dimensionless. $\xi(t)$ is assumed to be unbiased, *i.e.*, the average over noise realizations $\mathcal{E}[\cdots]$ gives zero, and the (dimensionless) correlation function α is assumed to be stationary,

$$\mathcal{E}[\xi(t)]=0,\quad \mathcal{E}[\xi(t)\xi(s)]=\alpha(t-s). \tag{10}$$

Assuming that there is no noise at the initial time, the initial conditions for $\rho(t)$ and $q_c(t)$ are

$$\begin{aligned}&\rho(0)=1,\qquad \dot{\rho}(0)=\ddot{\rho}(0)=0,\\&q_c(0)=0,\quad \dot{q}_c(0)=\ddot{q}_c(0)=0.\end{aligned} \tag{11}$$

We expand the auxiliary functions $\rho(t)$ and $q_c(t)$ in powers of λ,

$$\begin{aligned}&\rho(t)=\rho^{(0)}(t)+\lambda\rho^{(1)}(t)+O(\lambda^2),\\&q_c(t)=q_c^{(0)}(t)+\lambda q_c^{(1)}(t)+O(\lambda^2).\end{aligned} \tag{12}$$

The zeroth order (noiseless limit) is

$$\begin{aligned}&\rho^{(0)}(t)=1,\\&\ddot{q}_c^{(0)}(t)+\omega_0^2q_c^{(0)}(t)=\omega_0^2q_0(t),\end{aligned} \tag{13}$$

where $q_c^{(0)}(t)$ satisfies eqs. (7) and (8). At the final time $H(t_f)=p^2/2m+m\omega_0^2(x-d)^2/2$. The expectation value of $H(t_f)$ of the n-th mode for a realization of the noise $\xi(t)$ can be found exactly [39],

$$\begin{aligned}E_{n,\xi}\;=\;&\langle H(t_f)\rangle=\langle\Psi_n(t_f)|H(t_f)|\Psi_n(t_f)\rangle\\=\;&\frac{m}{2}\omega_0^2[q_c(t_f)-d]^2+\frac{\hbar\omega_0}{4}(2n+1)\frac{1+\rho^4(t_f)}{\rho^2(t_f)}\\&+\frac{m}{2}\dot{q}_c^2(t_f)+\frac{\hbar}{4\omega_0}(2n+1)\dot{\rho}^2(t_f).\end{aligned} \tag{14}$$

$E_{n,\xi}$ can be expanded in powers of λ as

$$E_{n,\xi}\approx E_{n,\xi}^{(0)}+\lambda E_{n,\xi}^{(1)}+\lambda^2E_{n,\xi}^{(2)}+\cdots. \tag{15}$$

The zeroth order is $E_{n,\xi}^{(0)}=\hbar\omega_0(n+\frac{1}{2})$, $E_{n,\xi}^{(1)}=0$, and the second order is

$$\begin{aligned}E_{n,\xi}^{(2)}\;=\;&\frac{1}{2}m\omega_0^2q_c^{(1)}(t_f)^2+\hbar\omega_0(2n+1)\rho^{(1)}(t_f)^2\\&+\frac{1}{2}m\dot{q}_c^{(1)}(t_f)^2+\frac{\hbar\dot{\rho}^{(1)}(t_f)^2}{4\omega_0}(2n+1).\end{aligned} \tag{16}$$

The noise sensitivity for a given transport protocol is defined as the second-order coefficient, so it has dimensions of energy [38],

$$\begin{aligned} G(t_f;n) &= \frac{1}{2}\mathcal{E}\left[\frac{\partial^2 E_{n,\xi}}{\partial\lambda^2}\right] = \mathcal{E}[E^{(2)}_{n,\xi}] \\ &= G_1 + G_2, \end{aligned} \tag{17}$$

where we have separated the terms that depend on ρ (static sensitivity) and q_c (dynamical sensitivity),

$$\begin{aligned} G_1 &= \hbar(2n+1)\left\{\omega_0\mathcal{E}[\rho^{(1)}(t_f)^2] + \frac{1}{4\omega_0}\mathcal{E}[\dot{\rho}^{(1)}(t_f)^2]\right\}, \\ G_2 &= \frac{1}{2}m\omega_0^2\mathcal{E}[q_c^{(1)}(t_f)^2] + \frac{1}{2}m\mathcal{E}[\dot{q}_c^{(1)}(t_f)^2]. \end{aligned} \tag{18}$$

For white noise, $\alpha(t) = \frac{D}{2}\delta(t)$, where D has dimensions of time and sets the strength of the noise [38]. The sensitivity becomes $G_W = G_{1W} + G_{2W}$,

$$G_{1W}(t_f) = \frac{D}{4}\hbar\omega_0^3 t_f(2n+1), \tag{19}$$

$$G_{2W}(t_f) = \frac{mD}{2}\int_0^{t_f} \mathrm{d}t\; [\ddot{q}_c^{(0)}(t)]^2. \tag{20}$$

The static sensitivity G_{1W} depends on final time and trap frequency, whereas the dynamical sensitivity G_{2W} depends on the transport trajectory and the mass of the ion. The static sensitivity may be reduced by shortening transport times with invariant-based engineering. We will design optimal trap trajectories to minimize the dynamical sensitivity for a given transport time. We define the mass and D-independent factor $F = \int_0^{t_f} \mathrm{d}t\; [\ddot{q}_c^{(0)}(t)]^2$ so that $G_{2W} = \frac{mD}{2}F$ and focus on minimizing F.

Optimal trajectory. –

Bound by Euler-Lagrange equation. Using a generalized Euler-Lagrange equation for F,

$$\frac{\partial L}{\partial q_c^{(0)}} - \frac{\mathrm{d}}{\mathrm{d}t}\frac{\partial L}{\partial \dot{q}_c^{(0)}} + \frac{\mathrm{d}^2}{\mathrm{d}t^2}\frac{\partial L}{\partial \ddot{q}_c^{(0)}} = 0, \tag{21}$$

where $L = [\ddot{q}_c^{(0)}(t)]^2$, the function $q_c^{(0)}$ satisfying $\mathrm{d}^4 q_c^{(0)}/\mathrm{d}t^4 = 0$ minimizes F for four boundary conditions for $q_c^{(0)}$ and $\dot{q}_c^{(0)}$ in eq. (7). Since we cannot impose the two additional boundary conditions in eq. (8), this gives the quasioptimal classical trajectory

$$q_c^{(0)} = d(3s^2 - 2s^3), \tag{22}$$

where $s = t/t_f$. This is the same trajectory found by minimizing the transient energy excitation (time average of potential energy without noise) in [26], see also [37]. It provides a lower bound for the sensitivity, as the set of functions satisfying four conditions is larger than the set satisfying six of them. This lower bound is

$$F_b = \frac{12d^2}{t_f^3}. \tag{23}$$

In the following, we shall find a sequence of protocols whose F tend to this lower bound.

Polynomial ansatz. Since the quasioptimal classical trajectory is a polynomial, we shall first check the sensitivity achieved with a higher-order polynomial satisfying the six boundary conditions in eqs. (7) and (8),

$$q_c^{(0)} = d(6s^5 - 15s^4 + 10s^3), \tag{24}$$

with $s = t/t_f$. This gives

$$F = \frac{120}{7}\frac{d^2}{t_f^3}, \tag{25}$$

which is $10/7 \approx 1.43$ times worse than the lower bound F_b in eq. (23). Higher-order polynomials with free parameters could be used to get closer to F_b. However, we find it convenient to approach F_b using a different ansatz.

Trigonometric functions protocol. For the ansatz [40]

$$\ddot{q}_c^{(0)}(t) = \sum_{j=1}^{N} b_j \sin\left(j\pi t/t_f\right), \tag{26}$$

the boundary conditions $\ddot{q}_c^{(0)}(0) = \ddot{q}_c^{(0)}(t_f) = 0$ are automatically satisfied. We integrate eq. (26) to specify the classical trajectory and velocity as

$$q_c^{(0)}(t) = \sum_{j=1}^{N} b_j \frac{t_f}{(j\pi)^2}\left[j\pi t - t_f\sin(j\pi t/t_f)\right], \tag{27}$$

$$\dot{q}_c^{(0)}(t) = \sum_{j=1}^{N} b_j \frac{t_f}{j\pi}\left[1 - \cos(j\pi t/t_f)\right]. \tag{28}$$

The initial conditions $q_c^{(0)}(0) = \dot{q}_c^{(0)}(0) = 0$ are automatically fulfilled. The final boundary conditions $q_c^{(0)}(t_f) = d$ and $\dot{q}_c^{(0)}(t_f) = 0$ give two conditions on the coefficients,

$$\sum_{j=1}^{N} b_j/j = d\pi/t_f^2, \quad \sum_{j=1}^{N} b_j[1-(-1)^j]/j = 0. \tag{29}$$

In principle, two parameters ($N = 2$) are enough to solve eq. (29). However, additional parameters ($N > 2$) can be used to minimize the function $F(b_1, b_2, \ldots, b_N) = \int_0^{t_f} \mathrm{d}t[\ddot{q}_c^{(0)}(t)]^2$. Using

$$\begin{aligned} \frac{\partial F(b_1, b_2, \cdots, b_N)}{\partial b_1} &= 0, \\ \frac{\partial F(b_1, b_2, \cdots, b_N)}{\partial b_2} &= 0, \\ &\vdots \\ \frac{\partial F(b_1, b_2, \cdots, b_N)}{\partial b_N} &= 0, \end{aligned} \tag{30}$$

the parameters can be found analytically. Interestingly, all the odd coefficients b_j ($j = 2k+1$) are 0.

In table 1, we give all the even coefficients that optimize F for the subset of trigonometric functions corresponding

Table 1: The optimal coefficients and F for different N, and f is the scale factor $f = Ft_f^3/d^2$.

N	b_2	b_4	b_6	b_8	b_{10}	b_{12}	F	f
2	$\frac{2\pi d}{t_f^2}$						$\frac{2\pi^2 d^2}{t_f^3}$	19.73
4	$\frac{8\pi d}{5t_f^2}$	$\frac{4\pi d}{5t_f^2}$					$\frac{8\pi^2 d^2}{5t_f^3}$	15.79
6	$\frac{72\pi d}{49t_f^2}$	$\frac{36\pi d}{49t_f^2}$	$\frac{24\pi d}{49t_f^2}$				$\frac{72\pi^2 d^2}{49t_f^3}$	14.50
8	$\frac{288\pi d}{205t_f^2}$	$\frac{144\pi d}{205t_f^2}$	$\frac{96\pi d}{205t_f^2}$	$\frac{72\pi d}{205t_f^2}$			$\frac{288\pi^2 d^2}{205t_f^3}$	13.86
10	$\frac{7200\pi d}{5269t_f^2}$	$\frac{3600\pi d}{5269t_f^2}$	$\frac{2400\pi d}{5269t_f^2}$	$\frac{1800\pi d}{5269t_f^2}$	$\frac{1440\pi d}{5269t_f^2}$		$\frac{7200\pi^2 d^2}{5269t_f^3}$	13.48
12	$\frac{7200\pi d}{5369t_f^2}$	$\frac{3600\pi d}{5369t_f^2}$	$\frac{2400\pi d}{5369t_f^2}$	$\frac{1800\pi d}{5369t_f^2}$	$\frac{1440\pi d}{5369t_f^2}$	$\frac{1200\pi d}{5369t_f^2}$	$\frac{7200\pi^2 d^2}{5369t_f^3}$	13.23

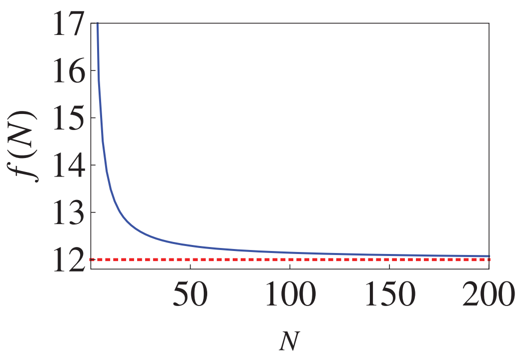

Fig. 1: The values of $f(N)$ *vs.* N as shown in eq. (32). The dashed red line is the limit 12.

to a given N. Note in particular that for three terms ($N = 6$) the optimal F for the trigonometric ansatz is 1.21 times worse than F_b, so it is better than the polynomial ansatz with the same number of terms. We denote the optimal F in each subset (of trigonometric functions) by $F(N)$. $F(N)$ is proportional to d^2/t_f^3 by a numerical factor $f(N)$,

$$F(N) = f(N)\frac{d^2}{t_f^3}. \tag{31}$$

By inspection of the expression of $b_2 = 2d\pi/t_f^2 - \sum_{k=2}^{N/2}\frac{1}{k}b_{2k}$ given by eq. (29) and the relations between b_{2k}, we find the general form of $f(N)$,

$$f(N) = 2\pi^2/H_{\frac{N}{2},2}, \tag{32}$$

where $H_{\frac{N}{2},2} = \sum_{k=1}^{N/2}\frac{1}{k^2}$ is a "harmonic number". When $N \to \infty$, $H_{\frac{N}{2},2} \to \pi^2/6$, and $f \to 12$, see fig. 1, which is the lower bound of f.

In fig. 2 we depict $q_c^{(0)}$ and q_0 for different N, as well as the lines for the bound protocol, whose q_0 is discontinuous at initial and final times. Clearly, with increasing N, the trap trajectories approach the trajectory for the bound.

For the N-dependent optimal protocols, the dynamical sensitivity G_{2W} is

$$G_{2W}(t_f;N) = \frac{Dm}{2}f(N)\frac{d^2}{t_f^3}, \tag{33}$$

and the total sensitivity will be

$$G_W(t_f;N) = \frac{D}{2}\left[\hbar\omega_0^3 t_f(n+\frac{1}{2}) + mf(N)\frac{d^2}{t_f^3}\right]. \tag{34}$$

While the dynamical sensitivity increases by shortening the shuttling times, the static (trajectory-independent) one decreases, so we also find optimal shuttling times that minimize the global (static plus dynamical) sensitivity using $\partial G_W/\partial t_f = 0$,

$$t_{fo} = \left[\frac{3\,\mathrm{m}f(N)d^2}{\hbar\omega_0^3(n+1/2)}\right]^{1/4}, \tag{35}$$

which is an optimal time to get the minimal value of the sensitivity $G_W(N)$. For large N this tends to

$$t_{fb} = \left[\frac{36\,\mathrm{m}d^2}{\hbar\omega_0^3(n+1/2)}\right]^{1/4}. \tag{36}$$

Summary and discussion. – In this paper we have found optimal trap trajectories to shuttle individual ions with noisy traps, specifically with white noise in the spring constant. The figure of merit we have used is the sensitivity, namely, the energy excitation. We have worked out a

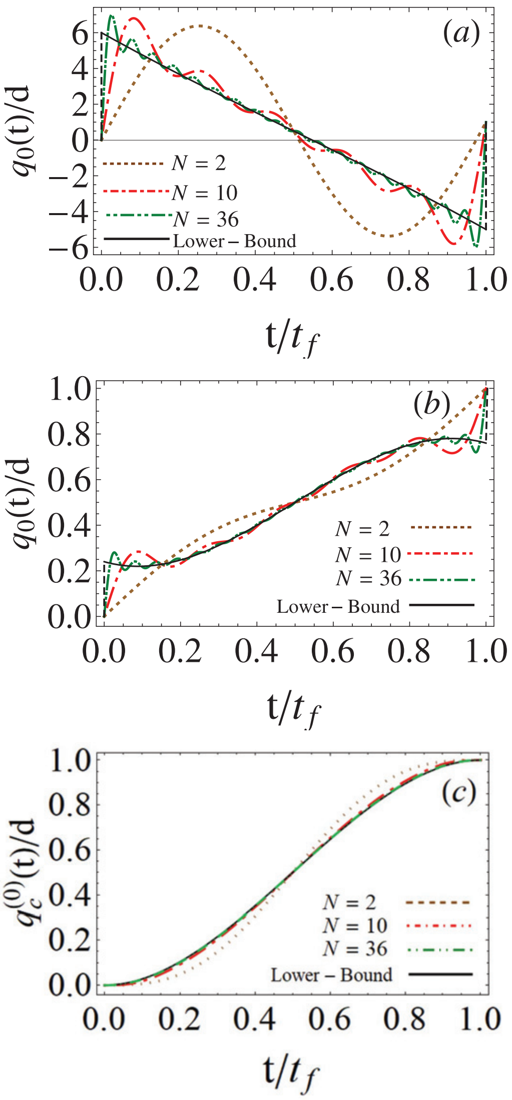

Fig. 2: $q_c^{(0)}(t)$ and $q_0(t)$ *vs.* t for different N. (a) $t_f = 1/\omega_0$; (b) $t_f = 5/\omega_0$; (c) the quasioptimal trajectory and the one for $N = 36$ are almost indistinguishable in the scale of the figure.

family of continuous protocols to approach the bound in the sensitivity provided by an optimal discontinuous trap trajectory. The sensitivity includes terms with opposite behavior with respect to the shuttling time and optimal shuttling times are also found.

While we have focused on white noise, it is interesting to see the effect of non-zero correlation times using the more general Ornstein-Uhlenbeck (OU) noise [39,46] when implementing these continuous trajectories. The excitation factor f defined as $f \equiv \frac{2t_f^3}{d^2 Dm} G_{2OU}$ for OU noise is plotted in fig. 3, see the appendix. As the correlation time τ approaches zero, it converges to the white-noise result, $f \to 12$. The excitation decreases by increasing the correlation time both for static and dynamical contributions, a trend also noted by Lu *et al.* in [39] for non-optimized trajectories.

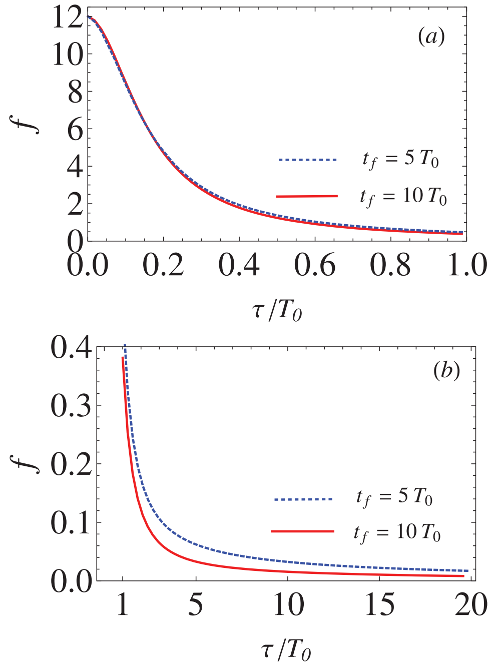

Fig. 3: The dashed blue line ($t_f = 5T_0$) and the solid red line ($t_f = 10T_0$) represent f of OU noise using quasioptimal trajectories in eq. (22). $T_0 = 2\pi/\omega_0$.

The current methodology to deal with noisy drivings could be extended to other operations such as fast separations [47] or merging [48] of atom chains, expansions [49] or rotations [50–52].

* * *

This work was supported by Basque Government Grant No. IT1470-22; the National Natural Science Foundation of China (Grant No. 12104390); Grant PID2021-126273NB-100 funded by MCIN/AEI/10.13039/501100011033, and by "ERDF A way of making Europe".

Data availability statement: All data that support the findings of this study are included within the article (and any supplementary files).

Appendix. –

OU noise sensitivity for the quasioptimal protocol. For Ornstein-Uhlenbeck noise, the correlation function decays exponentially, $\alpha(t) = \frac{D}{2\tau} e^{-t/\tau}$ [39], and the sensitivity in eq. (18) becomes [39]

$$\begin{aligned} G_{1OU} &= \hbar\omega_0^3(n+1/2)\int_0^{t_f}\alpha(s)(t_f-s)\cos(2\omega_0 s)\mathrm{d}s, \\ G_{2OU} &= m\int_0^{t_f}\mathrm{d}t\alpha(t)\cos(\omega_0 t)\int_0^{t_f-t}\mathrm{d}u\ddot{q}_c^{(0)}(u)\ddot{q}_c^{(0)}(u+t). \end{aligned} \tag{A.1}$$

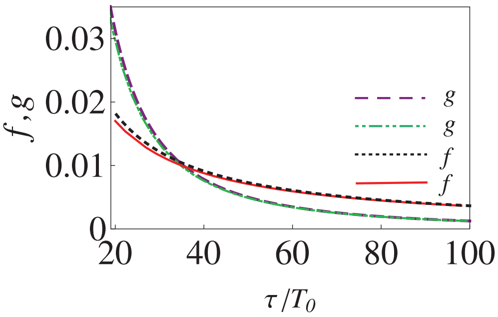

Fig. 4: The solid red line and the green dot-dashed line represent f and g of OU noise using quasioptimal trajectories in eq. (22). The dashed black line is the limit of f for large correlation times in eq. (A.10) and the purple long-dashed line is g for large correlation times in eq. (A.4). Other parameters: $\omega_0 = 2\pi/T_0$, $t_f = 5T_0$.

In the following, we will discuss G_{1OU} and G_{2OU} as a function of τ.

G_{1OU} can be calculated as

$$G_{1OU} = \frac{D}{4t_f}\hbar\omega_0(2n+1)g, \tag{A.2}$$

where

$$g = \frac{\omega_0^2\tau t_f}{(1+4\tau^2\omega_0^2)^2} \times \left[\frac{t_f}{\tau} - 1 + 4\tau^2\omega_0^2\left(1+\frac{t_f}{\tau}\right) + e^{-t_f/\tau}(1-4\tau^2\omega_0^2)\right]. \tag{A.3}$$

For $\tau \to 0$, the OU noise tends to white noise and $g = \omega_0^2 t_f$ which is the white-noise limit. When $\tau \gg T_0$, we have

$$g = \begin{cases} \dfrac{t_f \sin^2(\omega_0 t_f)}{2\tau}, & \omega_0 t_f \neq k\pi \\ \dfrac{t_f^2}{2\tau^2}, & \omega_0 t_f = k\pi. \end{cases} \tag{A.4}$$

For $k = 0, \pm1, \pm2, \dots, g \to 0$ as $\tau \to \infty$, see fig. 4.

Using the quasioptimal protocol for white noise given in eq. (22), the dynamical sensitivity can be calculated as

$$G_{2OU} = \frac{mDd^2}{2t_f^3} f, \tag{A.5}$$

where

$$f = \frac{12}{(1+X^2)^4}\left\{M_1 + e^{-\frac{t_f}{\tau}}[M_2\cos(\omega_0 t_f) + M_3 \sin(\omega_0 t_f)]\right\}, \tag{A.6}$$

with M_1, M_2 and M_3 given by

$$M_1 = 12\left(\frac{\tau}{t_f}\right)^3 (X^4 - 6X^2 + 1) + 3\frac{\tau}{t_f}(X^6 + X^4 - X^2 - 1) + (X^2+1)^3, \tag{A.7}$$

$$M_2 = -12\left(\frac{\tau}{t_f}\right)^3 (X^4 - 6X^2 + 1) + 12\left(\frac{\tau}{t_f}\right)^2 (3X^4 + 2X^2 - 1) + 3\frac{\tau}{t_f}(X^6 + X^4 - X^2 - 1), \tag{A.8}$$

$$M_3 = -48\left(\frac{\tau}{t_f}\right)^3 (X^3 - X) + 6\left(\frac{\tau}{t_f}\right)^2 (6X + 4X^3 - 2X^5) + 6\frac{\tau}{t_f}X(1+X^2)^2, \tag{A.9}$$

where $X = \omega_0\tau$. When τ tends to 0, $e^{-t_f/\tau} \to 0$ and $X \to 0$, so the dynamical sensitivity goes to the white-noise limit, $f = 12$.

For $\tau \gg T_0$, the sensitivity takes the form

$$f = \frac{72}{20\pi^2}\frac{T_0}{\tau}. \tag{A.10}$$

In summary, for the OU noise, increasing the correlation times reduces the effect of noise for both dynamical and static sensitivities, see fig. 4.

REFERENCES

[1] Wineland D. J., Monroe C., Itano W. M., Leibfried D., King B. E. and Meekhof D. M., *J. Res. Natl. Inst. Standards Technol.*, **103** (1998) 259.
[2] Pino J. M., Dreiling J. M., Figgatt C., Gaebler J. P., Moses S. A., Allman M., Baldwin C., Foss-Feig M., Hayes D., Mayer K. *et al.*, *Nature*, **592** (2021) 209.
[3] Moses S. A., Baldwin C. H., Allman M. S., Ancona R., Ascarrunz L., Barnes C., Bartolotta J., Bjork B., Blanchard P., Bohn M. *et al.*, *Phys. Rev. X*, **13** (2023) 041052.
[4] Palani D., Hasse F., Kiefer P., Boeckling F., Schroeder J.-P., Warring U. and Schaetz T., *Phys. Rev. A*, **107** (2023) L050601.
[5] Durandau J., Wagner J., Mailhot F., Brunet C.-A., Schmidt-Kaler F., Poschinger U. and Bérubé-Lauziére Y., *Quantum*, **7** (2023) 1175.
[6] Qi L., Chiaverini J., Espinós H., Palmero M. and Muga J. G., *EPL*, **134** (2021) 23001.
[7] Monroe C. and Kim J., *Science*, **339** (2013) 1164.
[8] Kaufmann P., Gloger T. F., Kaufmann D., Johanning M. and Wunderlich C., *Phys. Rev. Lett.*, **120** (2018) 010501.
[9] Bruzewicz C. D., Chiaverini J., McConnell R. and Sage J. M., *Appl. Phys. Rev.*, **6** (2019) 021314.
[10] Kaushal V., Lekitsch B., Stahl A., Hilder J., Pijn D., Schmiegelow C., Bermudez A., Müller M., Schmidt-Kaler F. and Poschinger U., *AVS Quantum Sci.*, **2** (2020) 014101.
[11] Häffner H., Roos C. and Blatt R., *Phys. Rep.*, **469** (2008) 155.
[12] Malinowski M., Allcock D. and Ballance C., *PRX Quantum*, **4** (2023) 040313.
[13] Ladd T. D., Jelezko F., Laflamme R., Nakamura Y., Monroe C. and O'Brien J. L., *Nature*, **464** (2010) 45.

[14] Linke N. M., Maslov D., Roetteler M., Debnath S., Figgatt C., Landsman K. A., Wright K. and Monroe C., *Proc. Natl. Acad. Sci.*, **114** (2017) 3305.

[15] Debnath S., Linke N. M., Figgatt C., Landsman K. A., Wright K. and Monroe C., *Nature*, **536** (2016) 63.

[16] Wolf F. and Schmidt P. O., *Measurement: Sensors*, **18** (2021) 100271.

[17] Ruster T., Kaufmann H., Luda M. A., Kaushal V., Schmiegelow C. T., Schmidt-Kaler F. and Poschinger U., *Phys. Rev. X*, **7** (2017) 031050.

[18] Wolf F., *Phys. Rev. Lett.*, **132** (2024) 083202.

[19] Wineland D. J. and Leibfried D., *Laser Phys. Lett.*, **8** (2011) 175.

[20] Rodriguez-Prieto A., Martínez-Garaot S., Lizuain I. and Muga J. G., *Phys. Rev. Res.*, **2** (2020) 023328.

[21] Martínez-Garaot S., Rodriguez-Prieto A. and Muga J., *Phys. Rev. A*, **98** (2018) 043622.

[22] Dupont-Nivet M., Westbrook C. and Schwartz S., *New J. Phys.*, **18** (2016) 113012.

[23] Guéry-Odelin D., Ruschhaupt A., Kiely A., Torrontegui E., Martínez-Garaot S. and Muga J. G., *Rev. Mod. Phys.*, **91** (2019) 045001.

[24] Torrontegui E., Ibáñez S., Martínez-Garaot S., Modugno M., del Campo A., Guéry-Odelin D., Ruschhaupt A., Chen X. and Muga J. G., *Advances in Atomic, Molecular, and Optical Physics*, Vol. **62** (Elsevier) 2013, pp. 117–169.

[25] Blatt R. and Wineland D., *Nature*, **453** (2008) 1008.

[26] Torrontegui E., Ibáñez S., Chen X., Ruschhaupt A., Guéry-Odelin D. and Muga J. G., *Phys. Rev. A*, **83** (2011) 013415.

[27] An S., Lv D., Del Campo A. and Kim K., *Nat. Commun.*, **7** (2016) 12999.

[28] Guéry-Odelin D. and Muga J. G., *Phys. Rev. A*, **90** (2014) 063425.

[29] Walther A., Ziesel F., Ruster T., Dawkins S. T., Ott K., Hettrich M., Singer K., Schmidt-Kaler F. and Poschinger U., *Phys. Rev. Lett.*, **109** (2012) 080501.

[30] Sterk J. D., Coakley H., Goldberg J., Hietala V., Lechtenberg J., McGuinness H., McMurtrey D., Parazzoli L. P., Van Der Wall J. and Stick D., *npj Quantum Inf.*, **8** (2022) 68.

[31] Hauck S. H., Alber G. and Stojanović V. M., *Phys. Rev. A*, **104** (2021) 053110.

[32] Palmero M., Bowler R., Gaebler J. P., Leibfried D. and Muga J., *Phys. Rev. A*, **90** (2014) 053408.

[33] Bowler R., Gaebler J., Lin Y., Tan T. R., Hanneke D., Jost J. D., Home J. P., Leibfried D. and Wineland D. J., *Phys. Rev. Lett.*, **109** (2012) 080502.

[34] An S., Lv D., Del Campo A. and Kim K., *Nat. Commun.*, **7** (2016) 12999.

[35] Coopmans L., Campbell S., De Chiara G. and Kiely A., *Phys. Rev. Res.*, **4** (2022) 043138.

[36] Whitty C., Kiely A. and Ruschhaupt A., *Phys. Rev. A*, **105** (2022) 013311.

[37] Lu X.-J., Muga J. G., Chen X., Poschinger U. G., Schmidt-Kaler F. and Ruschhaupt A., *Phys. Rev. A*, **89** (2014) 063414.

[38] Lu X.-J., Ruschhaupt A. and Muga J. G., *Phys. Rev. A*, **97** (2018) 053402.

[39] Lu X.-J., Ruschhaupt A., Martínez-Garaot S. and Muga J. G., *Entropy*, **22** (2020) 262.

[40] Espinós H., Echanobe J., Lu X.-J. and Muga J. G., *Philo. Trans. R. Soc.*, **380** (2022) 20210269.

[41] Lau H.-K. and James D. F., *Phys. Rev. A*, **83** (2011) 062330.

[42] Palmero M., Torrontegui E., Guéry-Odelin D. and Muga J. G., *Phys. Rev. A*, **88** (2013) 053423.

[43] Lewis H. R. and Riesenfeld W. B., *J. Math. Phys.*, **10** (1969) 1458.

[44] Lewis H. R. and Leach P. G. L., *J. Math. Phys.*, **23** (1982) 2371.

[45] Dhara A. K. and Lawande S. V., *J. Phys. A: Math. Gen.*, **17** (1984) 2423.

[46] Kiely A., *EPL*, **134** (2021) 10001.

[47] Palmero M., Martínez-Garaot S., Poschinger U. G., Ruschhaupt A. and Muga J. G., *New J. Phys.*, **17** (2015) 093031.

[48] Sutherland R. T., Burd S. C., Slichter D. H., Libby S. B. and Leibfried D., *Phys. Rev. Lett.*, **127** (2021) 083201.

[49] Torrontegui E., Chen X., Modugno M., Ruschhaupt A., Guéry-Odelin D. and Muga J., *Phys. Rev. A*, **85** (2012) 033605.

[50] Lu X.-J., Lizuain I. and Muga J. G., *Quantum*, **6** (2022) 740.

[51] Lu X.-J., Palmero M., Lizuain I. and Muga J. G., *Entropy*, **24** (2022) 1694.

[52] Orozco-Ruiz M., Simsek S., Kulmiya S. A., Hile S. J., Hensinger W. K. and Mintert F., *Phys. Rev. A*, **108** (2023) 022601.